

Synthesis and Biodegradation of Nanogels as Delivery Carriers for Carbohydrate Drugs

Jung Kwon Oh, Daniel J. Siegwart, and Krzysztof Matyjaszewski*

Department of Chemistry, Carnegie Mellon University, 4400 Fifth Avenue, Pittsburgh, Pennsylvania 15213

Received April 5, 2007; Revised Manuscript Received August 7, 2007

Biodegradable nanogels loaded with rhodamine B isothiocyanate–dextran (RITC–Dx) as a model for water-soluble biomacromolecular drugs were prepared using atom-transfer radical polymerization (ATRP) in a cyclohexane inverse miniemulsion in the presence of a disulfide-functionalized dimethacrylate cross linker. UV–vis spectroscopy was used to characterize the extent of incorporation of RITC–Dx into the nanogels. The loading efficiency of RITC–Dx into the nanogels exceeded 80%. These nanogels were degraded into polymeric sols in a reducing environment to release the encapsulated carbohydrate drugs. The released carbohydrate biomolecules specifically interacted with concanavalin A in water, suggesting that the biodegradable nanogels could be used as carriers to deliver carbohydrate drugs that can be released upon degradation to bind to pathogens based on lectins.

Introduction

Water-swallowable microgels are cross-linked hydrogel particles that have a tunable chemical composition and a 3D physical structure enabling control over water content, mechanical properties, and biocompatibility.¹ Several methods have been applied for the preparation of effective microgel particles. One method involves the use of natural biopolymers possessing a high degree of functional groups that are utilized in further cross-linking reactions with additional functional cross linkers, resulting in the formation of biopolymer-based microgels (called biomicrogels). Examples include carbohydrate-based species such as chitosan-^{2,3} and hyaluronan-based⁴ microgels and poly-(amino acid)-based microgels.⁵ Another method utilizes photolithographic techniques,⁶ micromolding,⁷ and microfluidics.⁸ However, the general method for the preparation of well-defined microgel particles utilizes various heterogeneous polymerization reactions of hydrophilic water-soluble monomers in the presence of either difunctional or multifunctional cross linkers. These include photo and suspension,⁹ precipitation,^{10,11} and inverse (mini)emulsion polymerization.^{12–16}

Microgel particles offer unique advantages as effective polymer drug-delivery systems (DDS). They have tunable size from nanometers to several micrometers and a large surface area for multivalent bioconjugation.^{11,17} When the dimensions of microgels are in the submicrometer range, they are also known as nanogels.¹⁸ These nanogels may contain an interior network for the incorporation of biorelated molecules. Physical entrapment of bioactive molecules such as drugs,^{3,11,12} proteins,^{13,15,19} and DNA^{4,14} in the polymeric network and their *in vitro* release behavior have been extensively investigated for application as targeted delivery carriers for biomedical applications.

The incorporation of carbohydrates, such as model water-soluble macromolecular drugs, into microgels or nanogels and their release behavior was also examined.²⁰ Gel particles based on poly(*N*-isopropylacrylamide-*co*-allylamine) were prepared by precipitation polymerization, followed by the addition of glutaric dialdehyde in the presence of Texas Red-labeled dextran in water, resulting in the formation of dextran-loaded particles.

They then studied the controlled release of dextran markers under various physical conditions.²¹ Cross-linked poly(vinyl pyrrolidone) nanoparticles were prepared in the presence of fluorescein isothiocyanate-labeled dextran using a reverse micellar technique, and their release behavior as potential carriers for hydrophilic drugs was studied.²² However, most of these dextran-loaded particles have serious problems pertaining to non-biodegradability and non-sustained drug release.

Biodegradation offers several advantages, such as the facilitation of the controllable release of encapsulated molecules from the interior of microgels and the removal of empty vehicles after drug release. A significant amount of work has been directed toward the development of cross linkers functionalized with (bio)degradable linkages in order to implement the biodegradability of hydrogels and microgels. These include peptides,²³ anhydrides,²⁴ oligo(lactate) esters,²⁵ disulfides,²⁶ and acetals.^{15,27}

We recently reported the successful synthesis and functionalization of stable biodegradable cross-linked nanogels of well-controlled hydrophilic polymers by utilizing atom transfer radical polymerization (ATRP)²⁸ in an inverse miniemulsion in the presence of a disulfide-functionalized dimethacrylate (DMA) cross linker.²⁹ More recently, we prepared nanogels loaded with doxorubicin (Dox), an anticancer drug, and demonstrated the utility of these nanogels as useful biomaterials, in particular, as targeted drug-delivery carriers for biological and biomedical applications. We found that this method allowed for the preparation of materials with many useful features. These include (1) the preservation of a high degree of halide end-functionality to enable further chain extension to form functional block copolymers and functionalization with biorelated molecules, (2) biodegradability in a reducing environment to individual polymeric chains with a relatively narrow molecular weight distribution ($M_w/M_n < 1.5$), (3) the formation of a uniformly cross-linked network in the individual particles, which is anticipated to improve control over the release of encapsulated agents, (4) better properties, including the swelling ratio, degradation behavior, and colloidal stability, of particles prepared by ATRP compared to the properties of counterparts prepared by conventional free-radical inverse miniemulsion polymerization, and (5) enhancement of circulation time in the blood because the nanogel consists of poly(oligo(ethylene

* Corresponding author. E-mail: km3b@andrew.cmu.edu.

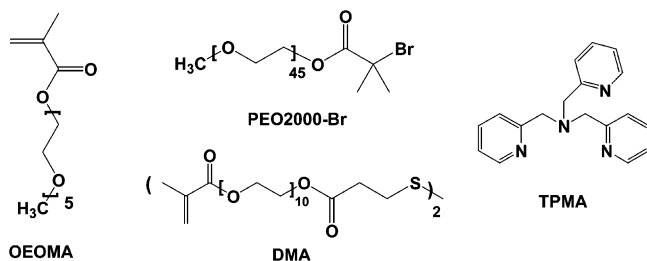
oxide)monomethyl ether methacrylate) (POEOMA), an analog of linear poly(ethylene oxide) (PEO) that can prevent nanoparticle uptake by the reticuloendothelial system (RES).³⁰ Furthermore, the nanogels were nontoxic to cells.

This article describes our further investigation of the application of nanogels as delivery carriers of carbohydrates as water-soluble biomacromolecular drugs. Rhodamine isothiocyanate-labeled dextran (RITC–Dx) was selected as a water-soluble biomacromolecular carbohydrate model drug. A series of stable RITC–Dx-loaded nanogels were prepared by inverse miniemulsion ATRP in the presence of RITC–Dx and DMA. The extent of incorporation of RITC–Dx into nanogels was characterized using UV–vis spectroscopy upon degradation of nanogels in the presence of water-soluble reducing agents. The release of RITC–Dx from nanogels was determined to demonstrate that the degradation triggers controllable release of encapsulated molecules. Last, specific binding of released RITC–Dx from nanogels upon degradation was demonstrated by interaction with lectins such as Concanavalin A (ConA) in water.

Experimental Section

Materials. OEOMA ($M = 300$ g/mol and pendent EO units DP ≈ 5) was purchased from Aldrich and purified by passing it through a column filled with basic alumina to remove the inhibitor. Copper(II) bromide (CuBr_2 , 99%) and L-ascorbic acid (AscA, 99+%) from Acros, sorbitan monooleate (Span 80), dithioerythritol (DTT, >99%), and cyclohexane (HPLC grade) from Aldrich, and glutathione (γ -Glu-Cys-Gly-OEt, reduced form) from Sigma were used as received without purification.

Tris[(2-pyridyl)methyl]amine (TPMA),³¹ dithiopropionyl poly(ethylene glycol) dimethacrylate (DMA),²⁹ and poly(ethylene oxide) (PEO)-functionalized bromoisobutyrate (PEO2000-Br, pendent EO units DP ≈ 45)³² were synthesized and purified as described elsewhere.



Instrumentation. Molecular weights of degraded polymers were determined by gel permeation chromatography (GPC), with THF as the eluent at 35 °C at a flow rate of 1 mL/min and linear poly(methyl methacrylate) (PMMA) standards for calibration. The detailed GPC measurements were described elsewhere.²⁹ Conversion was also determined using GPC by following the decrease of the macromonomer peak area relative to the increase in the polymer peak area. The particle size and size distribution were measured by dynamic light scattering (DLS) on a model HP5001 high-performance particle sizer from Malvern Instruments, Ltd. The sizes are expressed as $D_{av} \pm S$ (average diameter \pm standard deviation). Optical fluorescence microscopy (OFM) was carried out using a Zeiss Axiovert 200 microscope. A Rhod filter was used to image the RITC–dextran-loaded nanogels. UV–vis spectra were recorded in water on a Varian Cary 5000 UV–vis–NIR spectrophotometer using a 1-cm-wide quartz cuvette.

Synthesis of Nanogels Embedded with RITC–Dx. The detailed procedure for the preparation of cross-linked nanogel particles by activators generated by an electron-transfer (AGET) process for ATRP^{29,32–34} of OEOMA in a cyclohexane inverse miniemulsion at 30 °C in the presence of DMA cross linker was described elsewhere.²⁹

Using a similar procedure, a series of stable nanogels containing RITC–Dx were prepared in the presence of different amounts of RITC–Dx in the experiments. A typical procedure was as follows: OEOMA (1.4 g, 4.67 mmol), PEO2000–Br (33.4 mg, 0.016 mmol), DMA (286 mg, 0.064 mol), TPMA (2.3 mg, 0.008 mmol), CuBr_2 (1.7 mg, 0.008 mmol), RITC–Dx (95 mg, 6.8 wt % of OEOMA), and water (1.4 mL) were mixed in a 50 mL round-bottomed flask at room temperature. The resulting clear solution was mixed with a solution of Span 80 (1.0 g) in cyclohexane (20 g), and the mixture was sonicated for 2 min in an ice bath at 0 °C to form a stable inverse miniemulsion. The dispersion was transferred into a 50 mL Schlenk flask and then bubbled with nitrogen for 30 min. The flask was immersed in an oil bath preheated to 30 °C, and then an argon-purged aqueous solution of AscA (0.028 mmol/mL, 0.005 mmol, 200 μ L) was added via syringe to activate the catalyst and start the polymerization. The polymerization was stopped after 1.5 h by exposing the reaction mixture to air. A stable pink dispersion was obtained.

The cross-linked nanogels were purified by the addition of THF to the resulting dispersion, and then the resulting heterogeneous mixture was stirred at room temperature for 30 min. The nanogels were separated by centrifugation (15 000 rpm \times 20 min) at 4 °C. After the supernatant was removed, THF was added, and then the same procedure was repeated twice to completely remove THF-soluble species such as unreacted monomers and Span 80 (surfactant). After the final wash, the precipitate was dried in a vacuum oven at 30 °C for 2 h to yield pink nanogels.

Degradation of RITC–Dx-Containing Nanogels. Nanogels embedded with RITC–Dx were degraded in the presence of water-soluble reducing agents, including dithiothreitol (DTT) and glutathione at room temperature in water. For the use of DTT, dried, purified P(OEOMA) nanogels (34 mg) were stirred in water (3 mL) at room temperature for 24 h to allow them to be fully swollen. DTT (0.06 mL) was added to the dispersion of swollen gels and stirred at room temperature for 1 day to form a transparent pink solution. An aliquot of the mixture before and after degradation was taken for optical fluorescence microscopy analysis.

For the use of glutathione, a similar procedure was used, except for the use of purified nanogels (58.3 mg), glutathione (9.2 mg, 16 wt %), and PBS (3 mL). The resulting mixture was stirred for 3 h. The extent of degradation of the nanogels was determined by the weight ratio of swollen nanogels before and after the addition of glutathione.

Calibration Curves of RITC–Dx in Water. RITC–Dx (12 mg) was dissolved in PBS (5 mL) to form a transparent pink solution at a concentration of 2.4 mg/mL. Aliquots of the solution were diluted to RITC–Dx concentrations of 0.78, 0.48, and 0.22 mg/mL in PBS. Their UV–vis spectra were measured, and their absorbance at 555 nm was monitored to prepare a calibration curve.

Specific Binding between RITC–Dx Released from Nanogels and ConA. A clear stock solution of ConA at a concentration of 19.3 mg/mL was prepared by dissolving ConA (38.5 mg) in PBS (2 mL). The dried, purified nanogels containing 6.8% RITC–Dx (14.9 mg) were mixed with PBS (3.9 mL), and the resulting mixture was stirred at room temperature for 1 day. The concentration of polymer was 3.8 mg/mL, and the concentration of RITC–Dx was calculated to be 0.35 mg/mL. Glutathione (2.4 mg) was added, and the mixture was stirred at room temperature for 3 h to form a transparent pink solution. After the UV–vis spectrum of the solution was measured, an aliquot of the stock solution of ConA (0.5 g) was mixed and stirred at room temperature over several days. The transmittance at 700 nm was monitored from the UV–vis spectra of the mixture.

For comparison, a transparent mixture consisting of free RITC–Dx (17.6 mg) and PBS (3.8 mL) was prepared at a concentration of 4.66 mg/mL. An aliquot of the solution (0.2 mL) was diluted in PBS (3 mL) to a concentration of 0.36 mg/mL, and its UV–vis spectrum was measured. An aliquot of the stock solution of ConA (0.5 g) was added to the solution and stirred at room temperature. Similarly, the transmittance at 700 nm was monitored via UV–vis spectroscopy.

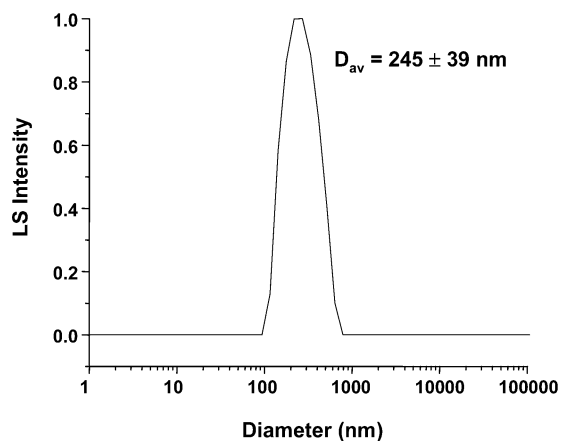


Figure 1. CONTIN plot of cross-linked POEOMA particles prepared by inverse miniemulsion AGET ATRP of OEOMA in cyclohexane in the presence of the DMA cross linker and RITC–Dx. Conditions: $[\text{OEOMA}]_0/[\text{PEO2000-Br}]_0/[\text{CuBr}_2/\text{TPMA}]_0/[\text{AscA}]_0 = 300/1/0.5/0.45$; $\text{OEOMA}/\text{water} = 1/1$ v/v; $[\text{DMA}]_0/[\text{PEO2000-Br}]_0 = 4/1$; RITC–Dx = 2.9 wt % of OEOMA; solids content = 10 wt %.

Results and Discussion

Synthesis of RITC–Dx-Containing Nanogels. Inverse miniemulsion AGET ATRP of OEOMA in cyclohexane was utilized for the preparation of biodegradable cross-linked POEOMA nanogels in the presence of a DMA cross linker at ambient temperature (30 °C).²⁹ A water-soluble PEO-based bromoisobutyrate macroinitiator (PEO2000-Br) was used to initiate the ATRP reactions. DMA was synthesized and used as a degradable cross linker at a DMA/PEO2000–Br ratio of 4.0/1. A water-soluble $\text{CuBr}_2/\text{TPMA}$ complex was used as an oxidatively stable precursor. Water-soluble AscA was used as a reducing agent that reacts with the Cu(II) catalyst complex to generate the corresponding active Cu(I) catalyst complex.

In the absence of DMA, droplets containing aqueous solutions of monomer become colloidal particles filled with swollen uncross-linked polymer chains. They had a narrow, monomodal size distribution of 151 ± 8 nm in diameter. The resulting POEOMA is well-controlled, with a narrow molecular weight distribution ($M_w/M_n < 1.3$).³⁴ In the presence of DMA, the resulting particles were not soluble in any solvents, including THF and water, indicating that the particles were cross linked during the polymerization. The diameter of particles dispersed in cyclohexane was 225 ± 24 nm. However, a small number of larger particles were detected.

To prepare nanogels entrapping RITC–Dx, different amounts of water-soluble RITC–Dx were introduced into the aqueous solution consisting of OEOMA, PEO2000–Br, $\text{CuBr}_2/\text{TPMA}$, DMA, and water. The resulting transparent pink solution was mixed with an organic solution of Span 80 in cyclohexane. The resulting binary mixture was sonicated in an ice bath at 0 °C to form a stable inverse miniemulsion of monomer droplets. An aqueous AscA solution was added to start polymerization at ambient temperature, resulting in the formation of pink dispersions of cross-linked RITC–Dx-containing P(OEOMA) particles.

In the presence of 2.9 wt % RITC–Dx of OEOMA, the particle size was 245 ± 39 nm in diameter as determined from DLS measurements, as shown in Figure 1. This diameter is larger than that of the particles prepared in the absence of RITC–Dx (225 ± 24 nm). When the isolated nanogels were redispersed in water and DLS was carried out in water, two populations were observed. The first peak (95% by volume)

corresponds to swollen nanogels (296 ± 65 nm), and the second peak (5% by volume) corresponds to aggregated nanogels (1540 ± 460 nm).

In the presence of 6.8 wt %, a similar diameter was observed. However, when the amount of RITC–Dx was further increased to 8.2 wt %, undissolved solids were observed in aqueous solution, indicating limited solubility of RITC–Dx in the monomer mixture; thus polymerization was not carried out under these conditions.

Degradation of RITC–Dx-Containing Nanogels. The purified RITC–Dx-containing nanogels were readily dispersed in water without the addition of extra surfactants. Figure 2a (left) shows the image for RITC–Dx-containing nanogels dispersed in water. Figure 2b shows a typical optical fluorescence microscopy (OFM) image of RITC–Dx-containing nanogel aggregates. The distinct bright spots on the dark background indicate that RITC–Dx molecules are localized in the nanogel particles.

Upon the addition of water-soluble dithiothreitol (DTT) as a reducing agent, the nanogels were degraded into individual polymeric chains. As a consequence, the turbid dispersion turned into the corresponding transparent solution (Figure 2a, right). In Figure 2c, the OFM image shows that a diffuse fluorescent signal in the background points out the release of RITC–dextran molecules from the nanogels. These results indicate that the degradation of nanogels could trigger the controllable release of the encapsulated carbohydrate drugs in a reducing environment through disulfide–thiol chemistry.

Glutathione is a tripeptide that is commonly found within cells. A few reports describe the use of glutathione as a water-soluble reducing agent that can degrade disulfide-containing polymers to the corresponding thiols.³⁵ In the experiments, the extent of degradation of the nanogel was determined by the weight loss of swollen nanogels in the presence of glutathione in water over time. It was observed that a significant amount (more than 88%) of nanogels containing RITC–Dx was degraded (or solubilized) within 3 h in the presence of 16 wt % glutathione. This result is comparative to that (89%) of nanogels prepared in the absence of RITC–Dx.

GPC measurements of the clear supernatant were then used to analyze polymers degraded from nanogels in the presence of glutathione. The solution containing degraded polymers could be filtered through a $0.2 \mu\text{m}$ filter without strong pressing, prior to its injection into the GPC, suggesting the formation of degraded linear polymers. In addition, the GPC trace indicated that degraded polymers had $M_n = 27\,800$ and $M_w/M_n = 1.4$.

Determination of the Extent of Incorporation of RITC–Dx into Nanogels. The above results indicate that a significant amount of RITC–Dx-containing nanogels (>88%) was degraded into individual polymeric chains upon addition of glutathione, resulting in the formation of a transparent solution in water. This led us to determine the degree of incorporation of RITC–Dx into nanogels using UV–vis spectroscopy. A calibration curve was first constructed from UV–vis spectra of various amounts of RITC–Dx in aqueous solutions (Figure 3a). As shown in Figure 3b, a linear plot of the absorbance at 555 nm versus the amount of RITC–Dx was obtained in water.

Next, a known amount of the purified dried RITC–Dx-containing nanogels was mixed with glutathione (15 wt % of nanogels) in water at room temperature for 1 day, resulting in the formation of a transparent pink solution upon degradation. Figure 3a (the upper spectrum) shows the UV–vis spectrum of the solution, where the maximum absorption was shifted by 3 nm from 555 to 558 nm. This is presumably due to a slight

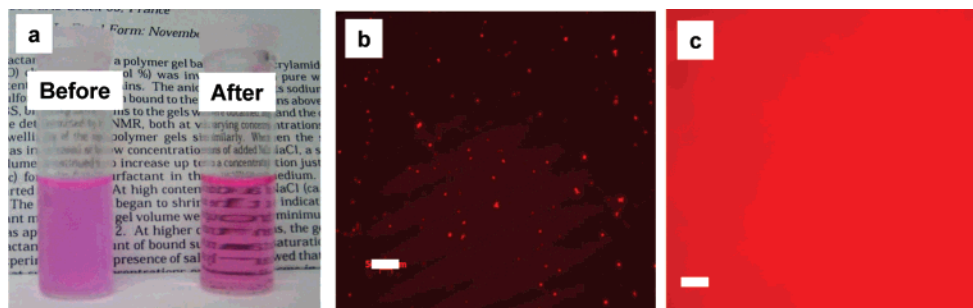


Figure 2. Images of nanogels containing RITC–dextran in water before and after the addition of dithiothreitol (DTT) (a) and optical fluorescence microscopy images of nanogel aggregates loaded with RITC–dextran before (b) and after (c) degradation in water. Thin films were spun cast onto a cleaned glass plate and dried at room temperature for 10 min. The scale bars in b and c are 50 μm .

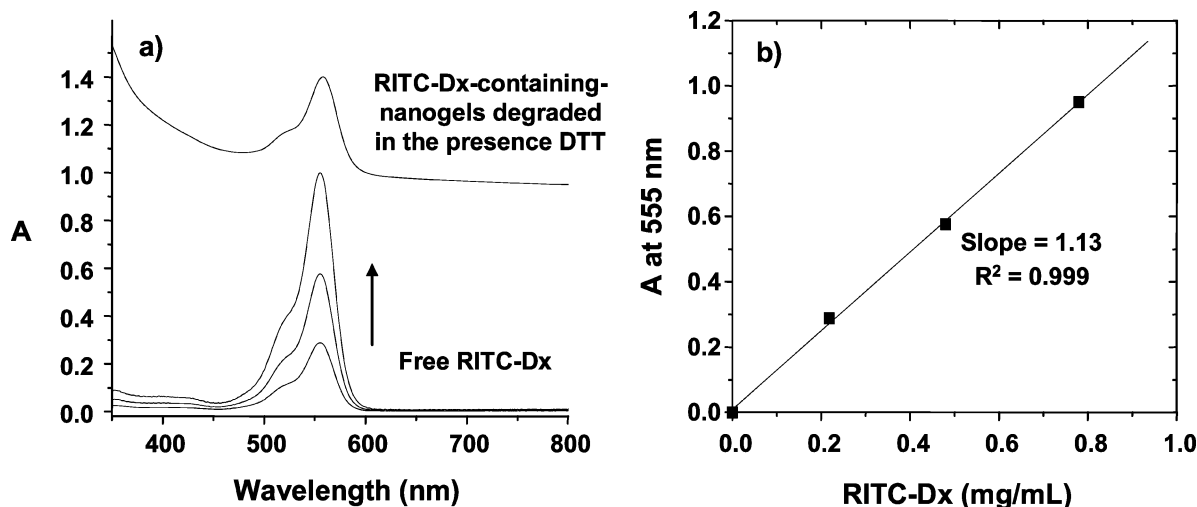


Figure 3. UV–vis spectra of free RITC–Dx at 0.78, 0.48, and 0.22 mg/mL and RITC–Dx-containing nanogels degraded in the presence of DTT in water (a) and the calibration curve of absorbance at 555 nm vs the amount of RITC–Dx (b). The UV–vis spectrum of degraded RITC–Dx-containing nanogels was shifted to produce a clear view.

Table 1. Extent of Incorporation of RITC–Dx in Nanogels Prepared by AGET ATRP of OEOMA in Cyclohexane Inverse Miniemulsion in the Presence of DMA and RITC–Dx at 30 $^{\circ}\text{C}$

RITC–Dx added to the polymerization (wt %)	incorporation	
	level (%) ^a	efficiency (%) ^b
2.9	4.0	84
6.8	9.1	81

^a Weight ratio of RITC–Dx to nanogels. ^b Weight ratio of RITC–Dx incorporated into nanogels to that added to the polymerization. Efficiency (%) = level/(amount of RITC–Dx added to polymerization/conversion). The amount of RITC–Dx added to the polymerization was calculated on the basis of monomer conversion to be 60% as determined by GPC measurements.

change in the polarity of the medium resulting from the presence of degraded POEOMA. From the absorbance at this wavelength and by using the calibration curve (Figure 3b), the amount of RITC–Dx embedded in nanogels was calculated. The results are presented in Table 1. Monomer conversion was taken into account when calculating the amount of RITC–Dx in the nanogels, reflected in both the amount added and incorporated. The efficiency was calculated using the following equation: efficiency % = level/(amount added to the polymerization/conversion). For nanogels prepared in the presence of 2.9 wt % RITC–Dx, the extent and efficiency of incorporation were 2.4 wt % and 84%, respectively. When the amount of RITC–Dx was increased from 2.9 to 6.8 wt %, the extent of incorporation was 5.5 wt %, resulting in a slight decrease in efficiency to 81%.

Specific Binding of RITC–Dx Released from Nanogels upon Degradation. The RITC–Dx-containing nanogels were

degraded in a reducing environment, and degradation triggered the release of carbohydrate drugs. The released carbohydrate molecules will bind to specific targets such as lectins. To assess the binding activity of RITC–Dx released from nanogels, Con A was selected as a target protein because it is a well-known protein that binds to glucose (homotetramer) at neutral pH.³⁶

A known amount of RITC–Dx-loaded nanogels was mixed with glutathione in PBS buffer for 1 day, resulting in the formation of a transparent solution upon degradation of over 95% nanogels. The transmittance (%T) at 700 nm of the solution was 93%, which is lower than 100% because of the presence of a small fraction of nondegraded nanogels. An aliquot of ConA solution was then added to the transparent solution and stirred at room temperature. The weight ratio of ConA/RITC–Dx was 7.0. The transmittance at 700 nm for the solution was monitored as a function of time, as shown in Figure 4. For comparison, a mixture consisting of a similar amount of free RITC–Dx and ConA in PBS buffer was also examined under similar conditions.

Figure 5 shows the transmittance at 700 nm versus time for the mixture consisting of released RITC–Dx, degraded nanogels, glutathione, and ConA in PBS buffer compared to the mixture consisting of free RITC–Dx in PBS buffer. Note that the amount of RITC–Dx in both solutions was the same, 0.36 mg/mL. It was found for both systems that the transmittance decreased with time and reached a plateau after 2 days. These results suggest the formation of aggregates caused by the interaction of RITC–Dx molecules with ConA, resulting in an increase in the turbidity of the mixtures. Large aggregates were

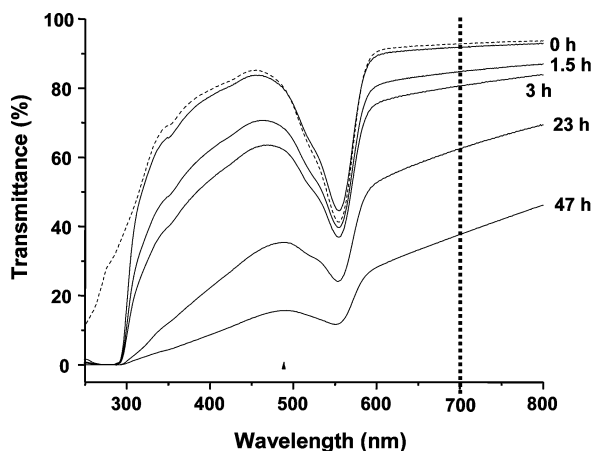


Figure 4. UV spectra recorded with the transmittance of a mixture consisting of RITC-dextran-containing nanogels and glutathione as a reducing agent before (uppermost dotted line) and after (solid lines) the addition of ConA in PBS as a function of time at 0, 1.5, 3, 23, and 47 h.

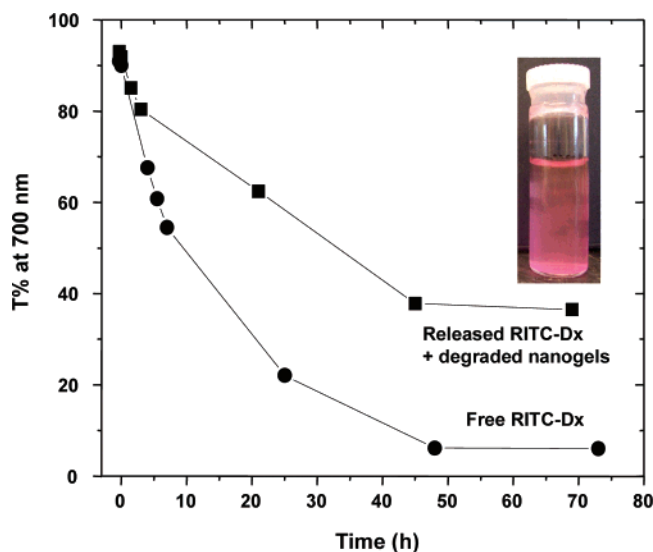


Figure 5. Transmittance at 700 nm vs time for a mixture of RITC-dextran released from nanogels upon degradation in the presence of glutathione compared with that of free RITC-Dx in PBS buffer. Image of the final dispersions showing the precipitation of aggregates (inset).

finally precipitated, as observed in the inset of Figure 5. These results imply that carbohydrate drugs released from nanogels upon degradation interact with the targeted proteins. However, the extent of interaction between RITC-Dx and ConA was somewhat lower in the presence of degraded polymers than in the absence of degraded polymers. For example, the transmittance was 39% for the mixture with degraded nanogels, compared to 7% for the mixture without nanogels after 2 days. This difference is probably due to incomplete degradation of RITC-Dx-loaded nanogels upon degradation in water. The dextran is still entrapped; therefore, these molecules cannot interact with ConA, reducing the number of interactions.

Conclusions

Stable nanogels entrapped with different amounts of RITC-Dx as model water-soluble biomacromolecular drugs were successfully prepared using ATRP in a cyclohexane inverse miniemulsion in the presence of RITC-Dx and DMA disulfide-

functionalized cross linker. The extent of incorporation of RITC-Dx into nanogels upon degradation of nanogels was characterized by UV-vis spectroscopy. The loading efficiency of RITC-Dx into nanogels exceeded 80%. Significant amounts of these nanogels (over 95%) were degraded into polymeric sols using water-soluble reducing agents, including DTT and biocompatible tripeptide glutathione. Release experiments demonstrated that degradation can trigger the controlled release of encapsulated carbohydrate drugs. The released carbohydrate biomolecules from nanogels upon degradation were able to interact specifically with proteins and lectins such as ConA in water.

These results suggest that nanogels could deliver carbohydrate drugs that could be released upon degradation in the presence of biocompatible glutathione to bind to pathogens based on lectins.

Acknowledgment. Support from the NSF (DMR 05-49353) is gratefully acknowledged. We thank Ke Min for the synthesis of the TPMA ligand and Dr. James Spanswick for helpful discussions. We also acknowledge Professor Jeffrey O. Hollinger for the use of the fluorescence microscope. J.K.O. thanks the Natural Sciences and Engineering Research Council (NSERC) of Canada for a postdoctoral fellowship.

References and Notes

- (1) (a) Langer, R.; Peppas, N. A. *AIChE J.* **2003**, *49*, 2990–3006. (b) Hoffman, A. S. *J. Controlled Release* **1987**, *6*, 297–305. (c) Peppas, N. A.; Hilt, J. Z.; Khademhosseini, A.; Langer, R. *Adv. Mater.* **2006**, *18*, 1345–1360.
- (2) (a) Bodnar, M.; Hartmann, J. F.; Borbely, J. *Biomacromolecules* **2006**, *7*, 3030–3036. (b) Rao, K. S. V. K.; Naidu, B. V. K.; Subha, M. C. S.; Sairam, M.; Mallikarjuna, N. N.; Aminabhavi, T. M. *Carbohydr. Polym.* **2006**, *66*, 345–351.
- (3) Zhang, H.; Mardiyani, S.; Chan, W. C. W.; Kumacheva, E. *Biomacromolecules* **2006**, *7*, 1568–1572.
- (4) Yun, Y. H.; Goetz, D. J.; Yellen, P.; Chen, W. *Biomaterials* **2003**, *25*, 147–157.
- (5) (a) Dinauer, N.; Balthasar, S.; Weber, C.; Kreuter, J.; Langer, K.; von Briesen, H. *Biomaterials* **2005**, *26*, 5898–5906. (b) Farrugia, C. A.; Groves, M. J. *J. Pharm. Pharmacol.* **1999**, *51*, 643–649.
- (6) Rolland, J. P.; Maynor, B. W.; Euliss, L. E.; Exner, A. E.; Denison, G. M.; DeSimone, J. M. *J. Am. Chem. Soc.* **2005**, *127*, 10096–10100.
- (7) (a) Franzesi, G. T.; Ni, B.; Ling, Y.; Khademhosseini, A. *J. Am. Chem. Soc.* **2006**, *128*, 15064–15065. (b) Yeh, J.; Ling, Y.; Karp, J. M.; Gantz, J.; Chandawarkar, A.; Eng, G.; Blumling, J., III; Langer, R.; Khademhosseini, A. *Biomaterials* **2006**, *27*, 5391–5398.
- (8) (a) Zhang, H.; Tumarkin, E.; Peerani, R.; Nie, Z.; Sullan, R. M. A.; Walker, G. C.; Kumacheva, E. *J. Am. Chem. Soc.* **2006**, *128*, 12205–12210. (b) Xu, S.; Nie, Z.; Seo, M.; Lewis, P.; Kumacheva, E.; Stone, H. A.; Garstecki, P.; Weibel, D. B.; Gitlin, I.; Whitesides, G. M. *Angew. Chem., Int. Ed.* **2005**, *44*, 724–728.
- (9) (a) Tsou, T.-L.; Tang, S.-T.; Huang, Y.-C.; Wu, J.-R.; Young, J.-J.; Wang, H.-J. *J. Mater. Sci.: Mater. Med.* **2005**, *16*, 95–100. (b) Arun, A.; Reddy, B. S. R. *Biomaterials* **2005**, *26*, 1185–1193. (c) Horak, D.; Svec, F.; Adamyan, A.; Titova, M.; Skuba, N.; Voronkova, O.; Trostenyuk, N.; Vishnevskii, V.; Gumargalieva, K. *Biomaterials* **1992**, *13*, 361–366. (d) Horak, D.; Rittich, B.; Spanova, A.; Benes, M. *J. Polymer* **2005**, *46*, 1245–1255. (e) Horak, D.; Svec, F.; Kalal, J.; Gumargalieva, K.; Adamyan, A.; Skuba, N.; Titova, M.; Trostenyuk, N. *Biomaterials* **1986**, *7*, 188–192.
- (10) (a) Zhang, J.; Xu, S.; Kumacheva, E. *J. Am. Chem. Soc.* **2004**, *126*, 7908–7914. (b) Berndt, I.; Pedersen, J. S.; Richtering, W. *Angew. Chem., Int. Ed.* **2006**, *45*, 1737–1741. (c) Kim, J.; Nayak, S.; Lyon, L. A. *J. Am. Chem. Soc.* **2005**, *127*, 9588–9592. (d) Duracher, D.; Elaissari, A.; Pichot, C. *J. Polym. Sci., Part A: Polym. Chem.* **1999**, *37*, 1823–1837. (e) Nayak, S.; Lee, H.; Chmielewski, J.; Lyon, L. A. *J. Am. Chem. Soc.* **2004**, *126*, 10258–10259. (f) Sinn, C. G.; Dimova, R.; Huin, C.; Sel, O.; Antonietti, M. *Macromolecules* **2006**, *39*, 9668. (g) Zhang, Y.; Guan, Y.; Zhou, S. *Biomacromolecules* **2006**, *7*, 3196–3201.
- (11) Das, M.; Mardiyani, S.; Chan, W. C. W.; Kumacheva, E. *Adv. Mater.* **2006**, *18*, 80–83.

- (12) Missirlis, D.; Tirelli, N.; Hubbell, J. A. *Langmuir* **2005**, *21*, 2605–2613.
- (13) Kwon, Y. J.; Standley, S. M.; Goh, S. L.; Frechet, J. M. J. *J. Controlled Release* **2005**, *105*, 199–212.
- (14) (a) Goh, S. L.; Murthy, N.; Xu, M.; Frechet, J. M. J. *Bioconjugate Chem.* **2004**, *15*, 467–474. (b) McAllister, K.; Sazani, P.; Adam, M.; Cho, M. J.; Rubinstein, M.; Samulski, R. J.; DeSimone, J. M. *J. Am. Chem. Soc.* **2002**, *124*, 15198–15207.
- (15) Murthy, N.; Xu, M.; Schuck, S.; Kunisawa, J.; Shastri, N.; Frechet, J. M. J. *Proc. Natl. Acad. Sci. U.S.A.* **2003**, *100*, 4995–5000.
- (16) (a) Braun, O.; Selb, J.; Candau, F. *Polymer* **2001**, *42*, 8499–8510. (b) Craparo, E. F.; Cavallaro, G.; Bondi, M. L.; Mandracchia, D.; Giammona, G. *Biomacromolecules* **2006**, *7*, 3083–3092.
- (17) Jung, T.; Kamm, W.; Breitenbach, A.; Kaiserling, E.; Xiao, J. X.; Kissel, T. *Eur. J. Pharm. Biopharm.* **2000**, *50*, 147–160.
- (18) (a) Sahiner, N.; Godbey, W. T.; McPherson, G. L.; John, V. T. *Colloid Polym. Sci.* **2006**, *284*, 1121–1129. (b) Kuckling, D.; Vo, C. D.; Adler, H. J. P.; Voelkel, A.; Coelfen, H. *Macromolecules* **2006**, *39*, 1585–1591.
- (19) Nolan, C. M.; Gelbaum, L. T.; Lyon, L. A. *Biomacromolecules* **2006**, *7*, 2918–2922.
- (20) Hu, Z.; Xia, X.; Marquez, M.; Weng, H.; Tang, L. *Macromol. Symp.* **2005**, *227*, 275–284.
- (21) Huang, G.; Gao, J.; Hu, Z.; St. John, J. V.; Ponder, B. C.; Moro, D. *J. Controlled Release* **2004**, *94*, 303–311.
- (22) (a) Bharali, D. J.; Sahoo, S. K.; Mozumdar, S.; Maitra, A. *J. Colloid Interface Sci.* **2003**, *258*, 415–423. (b) Gaur, U.; Sahoo, S. K.; De, T. K.; Ghosh, P. C.; Maitra, A.; Ghosh, P. K. *Int. J. Pharm.* **2000**, *202*, 1–10.
- (23) Plunkett, K. N.; Berkowski, K. L.; Moore, J. S. *Biomacromolecules* **2005**, *6*, 632–637; Kim, S.; Healy, K. E. *Biomacromolecules* **2003**, *4*, 1214–1223.
- (24) Muggli, D. S.; Burkoth, A. K.; Keyser, S. A.; Lee, H. R.; Anseth, K. S. *Macromolecules* **1998**, *31*, 4120–4125.
- (25) (a) Martens, P. J.; Bryant, S. J.; Anseth, K. S. *Biomacromolecules* **2003**, *4*, 283–292. (b) Eichenbaum, K. D.; Thomas, A. A.; Eichenbaum, G. M.; Gibney, B. R.; Needham, D.; Kiser, P. F. *Macromolecules* **2005**, *38*, 10757–10762. (c) Huang, X.; Lowe, T. L. *Biomacromolecules* **2005**, *6*, 2131–2139.
- (26) (a) Aliyar, H. A.; Hamilton, P. D.; Ravi, N. *Biomacromolecules* **2005**, *6*, 204–211. (b) Tsarevsky, N. V.; Matyjaszewski, K. *Macromolecules* **2005**, *38*, 3087–3092.
- (27) Murthy, N.; Thng, Y. X.; Schuck, S.; Xu, M. C.; Frechet, J. M. J. *J. Am. Chem. Soc.* **2002**, *124*, 12398–12399.
- (28) (a) Matyjaszewski, K.; Xia, J. *Chem. Rev.* **2001**, *101*, 2921–2990. (b) Kamigaito, M.; Ando, T.; Sawamoto, M. *Chem. Rev.* **2001**, *101*, 3689–3745. (c) Wang, J.-S.; Matyjaszewski, K. *J. Am. Chem. Soc.* **1995**, *117*, 5614–5615. (d) Matyjaszewski, K.; *Prog. Polym. Sci.* **2005**, *30*, 858–875. (e) Braunecker, W. A.; Matyjaszewski, K. *Prog. Polym. Sci.* **2007**, *32*, 93–146. (f) Tsarevsky, N. V.; Matyjaszewski, K. *Chem. Rev.* **2007**, *107*, 2270–2299. (g) Wang, J.-S.; Matyjaszewski, K. *Macromolecules* **1995**, *28*, 7901–7910. (h) Lee, S. B.; Russell, A. J.; Matyjaszewski, K. *Biomacromolecules* **2003**, *4*, 1386–1393.
- (29) (a) Oh, J. K.; Tang, C.; Gao, H.; Tsarevsky, N. V.; Matyjaszewski, K. *J. Am. Chem. Soc.* **2006**, *128*, 5578–5584. (b) Oh, J. K.; Siegwart, D. J.; Lee, H.-i.; Sherwood, G.; Peteanu, L.; Hollinger, J. O.; Kataoka, K.; Matyjaszewski, K. *J. Am. Chem. Soc.* **2007**, *129*, 5939–5945.
- (30) Seymour, L. W.; Duncan, R.; Strohalm, J.; Kopecek, J. *J. Biomed. Mater. Res., Part A* **1987**, *21*, 1341–1358.
- (31) (a) Tyeklar, Z.; Jacobson, R. R.; Wei, N.; Murthy, N. N.; Zubietta, J.; Karlin, K. D. *J. Am. Chem. Soc.* **1993**, *115*, 2677–2689. (b) Xia, J.; Matyjaszewski, K. *Macromolecules* **1999**, *32*, 2434–2437.
- (32) Oh, J. K.; Min, K.; Matyjaszewski, K. *Macromolecules* **2006**, *39*, 3161–3167.
- (33) (a) Jakubowski, W.; Matyjaszewski, K. *Angew. Chem., Int. Ed.* **2006**, *45*, 4482–4486. (b) Jakubowski, W.; Min, K.; Matyjaszewski, K. *Macromolecules* **2006**, *39*, 39–45. (c) Matyjaszewski, K.; Jakubowski, W.; Min, K.; Tang, W.; Huang, J.; Braunecker, W. A.; Tsarevsky, N. V. *Proc. Natl. Acad. Sci. U.S.A.* **2006**, *103*, 15309–15314.
- (34) Oh, J. K.; Perineau, F.; Matyjaszewski, K. *Macromolecules* **2006**, *39*, 8003–8010.
- (35) (a) Kakizawa, Y.; Harada, A.; Kataoka, K. *Biomacromolecules* **2001**, *2*, 491–497. (b) Li, C.; Madsen, J.; Armes, S. P.; Lewis, A. L. *Angew. Chem., Int. Ed.* **2006**, *45*, 3510–3513.
- (36) (a) Mortell, K. H.; Gingras, M.; Kiessling, L. L. *J. Am. Chem. Soc.* **1994**, *116*, 12053–12054. (b) Lu, C.; Chen, X.; Xie, Z.; Lu, T.; Wang, X.; Ma, J.; Jing, X. *Biomacromolecules* **2006**, *7*, 1806–1810. (c) Mammen, M.; Chio, S.-K.; Whitesides, G. M. *Angew. Chem., Int. Ed.* **1998**, *37*, 2755–2794. (d) Bae, W.-S.; Urban, M. W. *Biomacromolecules* **2006**, *7*, 1156–1161.

BM070381+